The Cryosphere Discuss., 6, 4101–4122, 2012
www.the-cryosphere-discuss.net/6/4101/2012/
doi:10.5194/tcd-6-4101-2012

The Cryosphere
Discussions

Brief communication
"Important role of the mid-tropospheric atmospheric circulation in the recent surface melt increase over the Greenland ice sheet"

X. Fettweis[1], **E. Hanna**[2], **C. Lang**[1], **A. Belleflamme**[1], **M. Erpicum**[1], **and H. Gallée**[3]

[1]Laboratory of Climatology, Department of Geography, University of Liège, Liège, Belgium
[2]Department of Geography, University of Sheffield, UK
[3]Laboratoire de Glaciologie et Géophysique de l'Environnement (LGGE), Grenoble, France

Received: 13 July 2012 – Accepted: 28 August 2012 – Published: 24 September 2012

Correspondence to: X. Fettweis (xavier.fettweis@ulg.ac.be)

Published by Copernicus Publications on behalf of the European Geosciences Union.

Abstract

Since 2007, there has been a succession of surface melt records over the Greenland Ice Sheet (GrIS) in continuity of the trend observed since the end of the 1990s towards increasing melt. But, these last two decades are characterized by an increase of negative phases of the North-Atlantic Oscillation (NAO) favouring warmer and drier summers than normal over GrIS. In this context, we use a circulation type classification based on the daily 500 hPa geopotential height to evaluate the role of the atmospheric dynamics in this surface melt acceleration since 20 yr. Due to the lack of direct observations, the interannual melt variability is gauged here by the summer (June-July-August) mean temperature at 700 hPa over Greenland; analogous atmospheric circulations in the past show that ~ 70 % of the 1992–2011 warming at 700 hPa over Greenland has been driven by changes in the atmospheric flow frequencies. Indeed, the occurrence of anticyclones in surface and at 500 hPa centred over the GrIS has doubled since the end of 1990s which induces southerly warm air advection along the Western Greenland coast and over the neighbouring Canadian islands. These changes in the NAO modes explain also why no significant warming has been observed these last five summers over Svalbard, where northerly atmospheric flows are more frequent than before. Therefore, the recent warmer summers over Greenland, Ellesmere and Baffin Islands can not be considered as a long term climate warming but are more rather a consequence of the NAO variability impacting the atmospheric heat transport. While no global model from the CMIP5 database projects consequent changes in NAO through this century, we can not exclude that these changes in NAO are due to global warming.

1 Introduction

Since 2007, we have observed over the Greenland Ice Sheet (GrIS) a succession of summers with record surface melt rates (Tedesco et al., 2008a,b, 2011; Rignot et al., 2011; Box et al., 2012; Hanna et al., 2012) coinciding with minimums in the Arctic sea ice cover (Serreze et al., 2007; Comiso et al., 2008). Except for 2009, the surface melt and runoff over 2007–2011 summers is unprecedented in the last 50 yr reanalysis-forced reconstructions (Van den Broeke et al., 2009; Fettweis et al., 2011b; Tedesco et al., 2011; Hanna et al., 2012). Initial indications at the time of writing (mid-July 2012) are that summer 2012 is following a similar near-record warm pattern. The recent melt records are in agreement with the trend observed since the end of 1990s over GrIs towards increasing melt (Mote, 2007; Fettweis et al., 2011b) which has been attributed to increased atmospheric greenhouse gas concentration (Fettweis, 2007; Hanna et al., 2008). This trend has also been observed in the Canadian Arctic Archipelago where the 2005–2009 melt was four times greater than the 1995–2000 mean (Gardner et al., 2011; Sharp et al., 2011; Fisher et al., 2012). But, paradoxically, no significant warming has been observed since 2004 over Svalbard located 500 km to the east of the GrIS. As a result, the increased mass loss rate observed from 1996 (Bamber et al., 2005) was no longer observed after 2004, and more recent Svalbard elevation change has been closer to balance (Moholdt et al., 2010).

This shows that the 2007–2011 warming recently observed over the GrIS did not occur everywhere in the Arctic and was therefore partly driven by anomalies in the atmospheric dynamics impacting the heat transport (Graversen et al., 2008; Mote, 1998) and notably by the North Atlantic Oscillation (NAO) and the related Greenland Blocking Index variability, as pointed out by Chylek et al. (2004), Fettweis et al. (2011a), Box et al. (2012) and Hanna et al. (2012). Indeed, the last five summers were characterized by persistent negative summer NAO modes favouring warmer and more anticyclonic conditions (drier) than normal over the GrIS (Box et al., 2012; Hanna et al., 2012) but, conversely, normal conditions over Svalbard as we will see later.

Therefore in this paper, we evaluate the role of the atmospheric dynamics in the 1992–2011 melt increase over GrIS and more generally of the warming of the atmosphere just over the GrIS surface (here at 700 hPa) in summer with the help of

- a Circulation Type Classification (CTC) extracting the main regimes of the mid-tropospheric general circulation. This allows us to show the changes in the atmospheric dynamics explaining the recent melt records over the GrIS.
- a flow-analogue method enabling us to estimate the part of the warming due to changes in atmospheric dynamics: it does this by reconstructing the climate of the last 20 summers with the help of analogue flows (i.e. similar tropospheric patterns) which occurred during the 1961–1990 summers. In theory, if we assume that the more recent 1992–2011 warming was driven solely by changes in atmospheric circulation, an equivalent warming should be reconstructed by replacing the current daily climate with that taken from the dates of analogous flows in the past.

2 The last two decades over Greenland in the last 50 yr perspective

As shown in Fig. 1a, the June-July-August (JJA) meltwater production over the GrIS has been increasing since 1995 and is without precedent in 1998, 2003, 2007, 2008, 2010 and 2011 compared with the last 50 yr. Over the last 20 yr (1992–2011), the amount of melt doubled compared with 1961–1990. Results from the regional climate model MAR (Fettweis et al., 2011b) forced by ERA-40 (1958–1978, Uppala et al., 2005) and ERA-INTERIM (1979–2011, Dee et al., 2011) reanalyses from the European Centre for Medium Range Weather Forecasts (ECMWF) are used here because no observations of meltwater production are available at the scale of the whole ice sheet. Only the melt extent can be derived from satellite (Fettweis et al., 2011b; Hanna et al., 2012) but, while melt extent and meltwater production are highly correlated (Fettweis et al., 2006), melt extent cannot be used as a direct proxy of meltwater production. Indeed, for the same melt extent, the amount of meltwater can be very different and depends on the presence and extent of bare ice zones (which have a lower albedo and higher melt rate than melting snow) in the melt area. However, the ability of MAR to simulate the melt extent has been shown in Fettweis et al. (2011b).

The MAR-based meltwater production variability is highly correlated (correlation coefficient of 0.93) with the JJA temperature at 700 hPa (T700) from the Reanalysis 1 (Kalnay et al., 1996) of the National Centers for Environmental Prediction (NCEP) and the National Center for Atmospheric Research (NCAR) averaged over an area covering the GrIS (70° W ≤ longitude ≤ 20° W and 60° N ≤ latitude ≤ 85° N). Here MAR is forced by the ECMWF reanalysis. The correlation of the melt with JJA NCEP-NCAR temperatures taken at other levels, including the ice sheet (near) surface temperature is less strong but still high (e.g. the correlation with the near-surface temperature is 0.85). Clearly JJA T700 does not explain all the melt variability because the melt amount is also affected by various factors including the winter accumulation, the snowpack behaviours induced by the previous summers and the snowfall occurring during summer (Tedesco et al., 2011). However, the most positive JJA T700 positive anomalies (1998, 2003,...) are synchronous with record melt years simulated by MAR (see Fig. 1a). Moreover, once normalized, the JJA T700 increase over the last 20 yr compares well with the melt increase. Finally, the daily variability of the temperature in the free atmosphere (here at 700 hPa) is more dependant on the atmospheric dynamics than the daily variability of the (near) surface temperature or melt which is impacted, for example, by the presence or absence of fresh snow at the surface and the inertia of the snowpack. This is why, we use T700 from the NCEP-NCAR reanalysis as a proxy for explaining the melt variability as it is independent of the MAR melt estimates, and so in the following analysis we discuss the recent warming at 700 hPa over Greenland instead of the surface melt increase.

In parallel with enhanced melt since the end of the 1990s, we observe an increase of the JJA geopotential height at 500 hPa (Z500) and the JJA sea level pressure (SLP) over the GrIS due to the increased occurrence of negative NAO phases in recent summers (see Fig. 1b). This means that the atmospheric dynamics in summer is currently more anticyclonic (at both the surface and 500 hPa) over GrIS than 20 yr ago, and this favours warm air advection along the Western GrIS due to weaker Icelandic lows, as shown in Fig. 2a and found by Hanna et al. (2012). Indeed, most of the significant temperature increase have occurred along the western coast of Greenland and on the Canadian Arctic Archipelago, while along the eastern coast – including the North Atlantic Ocean and Svalbard – the temperature changes are not statistically significant (Fig. 2a).

The Z500, T700, SLP used here come from the NCEP-NCAR reanalysis over 1958–2011. To check the dataset dependence of our results, we produced similar figures to Figs. 2 and 3 but this time based on the ECMWF ERA-40 (1958–1978) and ERA-INTERIM (1979–2011) reanalyses – see Supplement – although it is noted that the ECMWF-based time series (composed of two different reanalyses) is not homogeneous.

3 Methodology

3.1 Circulation type classification

The automatic CTC method used here is adapted from the approach of Lund (1963) in which each pair of days is characterized by a similarity index based on the daily Z500 and used afterwards to group days with similar circulations (Philipp et al., 2010). In the original classification of Lund (1963), the correlation between the SLP surfaces is used to evaluate the similarity between two days. Here, in view of the GrIS topography, it is better to use the Z500 surfaces (Z700 can reach altitudes bellow the ice sheet top). The correlation-based index treats two parallel but distant Z500 surfaces as similar because they have the same pattern. However, if the Z500 surfaces are at different heights, this means that the temperature of the troposphere below 500 hPa is different. Therefore, these two Z500 surfaces will not have the same impact on the surface melt and then, can not be considered as similar in our case. Hence our similarity index is more rather a function of the euclidean distance between the two Z500 surfaces, which gives more weight to the height of the Z500 surfaces in our CTC. But, Fettweis et al. (2011a) showed that the melt variability over the GrIS is driven more by the height of the Z500 surfaces than their pattern. We refer to Fettweis et al. (2011a) for more details about our CTC and the choice of our index. The only difference with Fettweis et al. (2011a) is the domain which has been enlarged here to include Svalbard and Ellesmere islands. In addition, instead of fixing to eight the number of circulation types allowed in our CTC as in Fettweis et al. (2011a), this number has been chosen to three here to only distinguish neutral, cyclonic and anticyclonic regimes.

3.2 Flow analogues

The flow-analogue method, used here for estimating the JJA temperature anomalies at 700 hPa induced by the general circulation, is similar to the one from Vautard and Yiou (2009) i.e. for each JJA day of the 1958–2011 period, flow analogues are selected in a 30-day window centred on this given day but not in the same year. As for the CTC, our similarity index (defined in the previous section) is used to select the most similar Z500 surfaces to a given day. Its value is chosen to have analogues in at least 10 different summers to avoid an abnormal summer being "described" by another abnormal summer and so that the analogues properly represent the average climate corresponding to a Z500 surface for a given date. With this aim, it is clear that the flow-analogue method cannot represent exceptional climate anomalies. In addition, since the aim is to estimate the impact of the atmospheric dynamics on the last 20 yr melt variability over the GrIS, analogues are only taken from 1961–1990 summers. The daily analogue T700 is then defined as the median of daily T700 from the analogue days. Using analogues in at least 5 or 15 summers instead of 10, 20-day or 40-day window instead of 30-day window, mean instead of the median of the analogue T700, daily anomalies instead of raw values, analogues taken in the 1958–2011 summers instead of 1961–1990 does not significantly affect our results, as shown in Supplement. The uncertainties given in our analogues-based results were derived using the different configurations listed above (see Table S1 in the Supplement).

Title Page
Abstract | Introduction
Conclusions | References
Tables | Figures
◀| |▶
◀ ▶
Back | Close
Full Screen / Esc
Printer-friendly Version
Interactive Discussion

4 Changes in atmospheric dynamics

The three main atmospheric circulation regimes extracted by our CTC are shown in Fig. 3 as Z500 anomalies in respect to the JJA Z500 mean. As Z500 depends on the atmospheric temperature below 500 hPa, the pattern of the corresponding T700 anomalies in each circulation type is obviously correlated to the Z500 one while, as we will show later, T700 does not drive our CTC. The main circulation types found by our automatic CTC are a type (no. 1) near the JJA climatology induced by neutral NAO conditions; a cyclonic types (no. 2) induced by positive NAO conditions and an anticyclonic type (no. 3) gauged by negative NAO phases. However, it should be noted that the last type groups the non-classified situations and is consequently less homogeneous. In average over the period 1958–2011, Type no. 1 occurs 49 % of the JJA time while only 19 % of JJA daily circulations is classified as anticyclonic (Type no. 3).

For the mid-1960s to mid-1990s, both CRU and CPC JJA NAO indexes are on average positive (see Fig. 3b), indicating more frequent cyclonic circulations at the expense of anticyclonic regimes. Before 1965, slightly negative NAO conditions prevailed in average, favouring anticyclonic types (see Fig. 3c), but those negative NAO phases are insignificant compared with those occurring since 2000. Indeed, over the two last decades, there was a significant increase from 15 % to 40 % (respectively decrease) of the anticyclonic Type no. 3 (respectively Types no. 1 and no. 2) favouring warmer conditions over Greenland and in particular along its western coast where warm air masses were advected from the south by the anticyclone, in full agreement with Fig. 2. However, since the atmospheric temperature impacts the geopotential height, the increase of occurrence of Type no. 3 could be an artefact driven by the atmospheric temperature increase over the last 20 yr. But, on the one hand, Fig. 1d shows that such a temperature increase occurs for each type of the CTC indicating that the variability of our circulation regimes is independent of the current warming. On the other hand, the same CTC based on SLP instead of Z500 shows that there is also an increase of anticyclonic conditions at surface, which favoured warmer atmospheric conditions in

West-Greenland (see Fig. S4 in the Supplement). Therefore, such an increase in the occurrence of anticyclonic conditions (both at surface and altitude) is not an artefact of our methodology and is in agreement with the statistically significant temperature increase since the 1990s over Greenland and the neighbouring Canadian islands (see the next section). Over Svalbard, the increasing occurrence of anticyclones centred over Greenland favours northerly flows inducing temperatures rather near the normal in agreement with Kvamsto et al. (2011) who showed that the highest temperatures over Svalbard were reached at the beginning of the 2000s.

5 Atmospheric dynamics induced warming

By using the flow analogues technique, we can evaluate the part of the currently observed warming over GrIS which is induced by anomalies in atmosphere dynamics independently of the anthropogenic radiative forcing. At a daily time scale, the Z500 surfaces and the corresponding Z500 analogues-based ones compare very well over 1992–2011, which validates our flow analogues technique. Indeed, if we average the Z500 surfaces over the area (described earlier) covering the GrIS and if we choose the Z500 analogues by using a similarity index computed only on this area, the correlation is 0.99 for a RMSE of 13.2 m knowing that the daily standard deviation is 74.2 m. We refer to the Supplement for a comparison in two dimensions (see Figs. S5 and S6). Such an agreement shows that the Z500 surfaces from the last two decades are not exceptional because analogues can be successfully found in the past. But let us remember that the occurrence of the anticyclone-like Z500 surfaces during the recent 2007–2011 summers is exceptional, as shown in the previous sections.

For T700 still averaged over this area, the correlation with the daily analogues-based T700 is 0.86 with a RMSE of 1.2 °C for a standard deviation of 2.3 °C over 1992–2011. It is clear that the comparison is worse for T700 than Z500 since for a same Z500 surface, T700 can be very different depending on whether there is a low or a high pressure at surface and on the temperature gradient in the airmass below 500 hPa. In addition, bearing in mind that the climate is currently warming due to the anthropogenic radiative forcing, the T700 associated to a Z500 surface was generally lower 20 yr ago than currently, according to Fig. 1d.

Figures 1e and 2b show the T700 increase induced by the changes in the general circulation using analogues from 1961–1990. The pattern of Fig. 2a is well reproduced by the analogues but the temperature increase is underestimated. Indeed, averaged over Greenland and after having applied a 10 yr running mean, the analogues explain only 70 ± 5 % (resp. 65 ± 5 %) of the reanalysis-based 1992–2011 (resp. 1982–2011) JJA warming at 700 hPa (see Fig. 1d) knowing that the linear trend of JJA T700 is 0.09 °C/summer (resp. 0.05 °C/summer). The global warming gauged here by the global annual 2 m temperature from the NCEP-NCAR reanalysis on which we have also applied a 10-yr running mean represents 27 % (resp. 34 %) of the NCEP-NCAR based 1992–2011 (resp. 1982–2011) JJA T700 linear increase. A similar ratio is also found in the ECMWF reanalysis while this time series is not homogeneous over the whole period (see Supplement). By adding the global annual 2 m temperature anomalies (in respect to 1961–1990) to the analogues based T700 time series, we explain 98 ± 5 % (resp. 100 ± 5 %) of the NCEP-NCAR based T700 warming. Without applying a 10-yr running mean to the time series, the reconstructions explain 93 % (resp. 104 %) of the NCEP-NCAR based T700 warming over 1992–2011 (resp. 1982–2011).

This fine agreement of our reconstructed T700 trends with the NCEP-NCAR based ones shows that our analogues approach provides a realistic estimate of the warming induced by changes in the general circulation independently of the anthropogenic radiative forcing. However, even if we are able to reconstruct the current trend of T700, we are not able to explain all the T700 JJA variability at an annual time scale based on T700 analogues from the past plus the global change. Indeed, since the state of the atmosphere is unique every day, using analogues from the past for explaining the current climate has limitations and can not reproduce exceptional summers like the cold summer of 1992 which resulted from the volcanic eruption of Mount Pinatubo (Abdalati and Steffen, 1997; Box, 2002; Hanna et al., 2005).

6 Circulation changes and global warming

Our use of past analogues means we do not directly reconstruct the melt increase, and the use of reanalysis instead of direct observations for detecting changes at 700 hPa over Greenland may be regarded as perhaps somewhat questionnable (Screen and Simmonds, 2011). However, in agreement with Graversen et al. (2008) and Hanna et al. (2012), our results imply an important role of the general circulation in the forcing recent GRIS record surface melt and runoff independently – to some degrees at least – of global warming and Arctic amplification (Serreze et al., 2009). Nevertheless, these recent changes in the circulation regimes could be an indirect consequence of climate change.

Indeed, Overland and Wang (2010) and Jaiser et al. (2012) showed that the recently observed sea ice retreat attributed in part to global warming (Serreze et al., 2007) influences the NAO modes in winter. Nevertheless, Fig. 4 seems to suggest that global warming projected by general circulation models (GCMs) from the CMIP5 (Coupled Model Intercomparison Project Phase 5) database does not greatly impact the NAO and general circulation in summer over Greenland as shown by Belleflamme et al. (2012). While we observe a sharp decrease of the NAO index over the last 10 yr, only one GCM (plotted in black in Fig. 4) projects such NAO negative values in future and the CMIP5 ensemble mean (composed of 28 GCMs listed in Supplement) rather projects a small NAO increase for both mid-range (RCP 4.5) and very pessimistic (RCP 8.5) scenarios through this century (see Fig. 4). Therefore, just how the future circulation regimes will be modified by ongoing climate change remains unclear and so this whole area needs much further research. In addition, the recent changes towards a more negative summer NAO are quite short-term in the climate context and could still yet be attributed to the "natural" variability.

7 Conclusions

With the help of a CTC, we have shown that anticyclonic conditions (at surface and in altitude) gauged by negative NAO indexes are two times more frequent in the last summers over Greenland compared with the last 50 yr. These anticyclones favour warmer conditions over Greenland and in particular along its western coast and the neighbouring Canadian islands (Ellesmere and Baffin), where they induce a northward flux, as found by Hanna et al. (2012). Over Svalbard, the Greenland anticyclones tend to rather instead induce a southward flux which explains why no melt record has recently been observed in Svalbard unlike Greenland located 500 km away. By using a flow analogues method, we have estimated the part of the 1992–2011 (resp. 1982–2011) summer warming simulated by the NCEP-NCAR reanalysis at 700 hPa over Greenland induced by these changes in the general circulation to be 70 ± 5 % (65 ± 5 %). The CMIP5 GCMs seem to suggest that these atmospheric circulation anomalies do not result from the global warming.

The next step as future development is to study in more depth the impact of a warmer climate on the general circulation as well as to evaluate the role played by the general circulation in the current warming observed at the whole-Arctic scale (Graversen et al., 2008; Serreze et al., 2009).

Supplementary material related to this article is available online at: http://www.the-cryosphere-discuss.net/6/4101/2012/tcd-6-4101-2012-supplement.pdf.

Acknowledgements. Xavier Fettweis is a postdoctoral researcher of the Belgian National Fund for Scientific Research. We thank the European Centre for Medium-Range Weather Forecasts (ECMWF) for the ERA-40/ERA-INTERIM reanalysis (http://www.ecmwf.int), the NOAA/OAR/ESRL PSD (Boulder, Colorado, US) for the NCEP/NCAR Reanalysis (http://www.esrl.noaa.gov/psd/), the NOAA Climate Prediction Center for its NAO index (http://www.cpc.

Title Page
Abstract
Introduction
Conclusions
References
Tables
Figures
◀◀
▶▶
◀
▶
Back
Close
Full Screen / Esc
Printer-friendly Version
Interactive Discussion

ncep.noaa.gov/) and the Climate Research Unit (CRU) for its NAO index (http://www.cru.uea.ac.uk/). For their roles in producing, coordinating, and making available the CMIP5 model output (http://cmip-pcmdi.llnl.gov/cmip5/), we acknowledge the climate modelling groups (listed in Supplement), the World Climate Research Programme's (WCRP) Working Group on Coupled Modelling (WGCM), and the Global Organization for Earth System Science Portals (GO-ESSP). Finally, this work was partly funded by the ANR CEPS "Green Greenland" project.

References

Abdalati, W. and K. Steffen: The apparent effects of the Mt. Pinatubo eruption on the Greenland ice sheet melt extent, Geophys. Res. Lett., 24, 1795–1797, doi:10.1029/97GL01706, 1997. 4110

Bamber, J. L., Krabill, W., Raper, V., Dowdeswell, J. A., and Oerlemans, J.: Elevation changes measured on Svalbard glaciers and ice caps from airborne laser data, Ann. Glaciol., 42, 202–208, 2005. 4103

Belleflamme, A., Fettweis, X., Lang, C., and Erpicum, M.: Current and future atmospheric circulation at 500 hPa over Greenland simulated by the CMIP3 and CMIP5 global models, Clim. Dynam., accepted, 2012. 4111

Box, J. E.: Survey of Greenland instrumental temperature records: 1873–2001, Int. J. Climatol., 22, 1829–1847, 2002. 4110

Box, J. E., Fettweis, X., Stroeve, J. C., Tedesco, M., Hall, D. K., and Steffen, K.: Greenland ice sheet albedo feedback: thermodynamics and atmospheric drivers, The Cryosphere, 6, 821–839, doi:10.5194/tc-6-821-2012, 2012. 4102, 4103

Chylek, P., Box, J., and Lesins, G.: Global warming and the Greenland ice sheet, Climatic Change, 63, 201–221, doi:10.1023/B:CLIM.0000018509.74228.03, 2004. 4103

Comiso, C., Parkinson, C. L., Gerttsen, R., and Stock, L.: Accelerated decline in the Arctic sea ice cover, Geophys. Res. Lett., 35, 01703, doi:10.1029/2007GL031972, 2008. 4103

Dee, D. P.; Uppala, S. M.; Simmons, A. J.; Berrisford, P.; Poli, P.; Kobayashi, S.; Andrae, U.; Balmaseda, M. A.; Balsamo, G.; Bauer, P.; Bechtold, P.; Beljaars, A. C. M.; van de Berg, L.; Bidlot, J.; Bormann, N.; Delsol, C.; Dragani, R.; Fuentes, M.; Geer, A. J.; Haimberger, L.; Healy, S. B.; Hersbach, H.; Hòlm, E. V.; Isaksen, L.; Kållberg, P.; Köhler, M.; Matricardi, M.; McNally, A. P.; Monge-Sanz, B. M.; Morcrette, J.-J.; Park, B.-K.; Peubey, C.; de Rosnay, P.;

Tavolato, C.; Thépaut, J.-N.; Vitart, F.: The ERA-Interim reanalysis: configuration and performance of the data assimilation system, Quart. J. R. Meteorol. Soc., 137, 553–597, 2011. 4104

Fettweis, X.: Reconstruction of the 1979–2006 Greenland ice sheet surface mass balance using the regional climate model MAR, The Cryosphere, 1, 21–40, doi:10.5194/tc-1-21-2007, 2007. 4103

Fettweis, X., Gallée, H., Lefebre, L., and van Ypersele, J.-P.: The 1988–2003 Greenland ice sheet melt extent by passive microwave satellite data and a regional climate model, Clim. Dynam., 27, 531–541, doi:10.1007/s00382-006-0150-8, 2006. 4104

Fettweis, X., Mabille, G., Erpicum, M., Nicolay, S., and van den Broeke, M.: The 1958–2009 Greenland ice sheet surface melt and the mid-tropospheric atmospheric circulation, Clim. Dynam., 36, 139–159, doi:10.1007/s00382-010-0772-8, 2011a. 4103, 4107

Fettweis, X., Tedesco, M., van den Broeke, M., and Ettema, J.: Melting trends over the Greenland ice sheet (1958–2009) from spaceborne microwave data and regional climate models, The Cryosphere, 5, 359–375, doi:10.5194/tc-5-359-2011, 2011b. 4103, 4104, 4105

Fisher, D., Zheng, J., Burgess, D., Zdanowicz, C., Kinnard, C., Sharp, M., Bourgeois, J.: Recent melt rates of Canadian arctic ice caps are the highest in four millennia, Global Planet. Change, 84–85, 3–7, doi:10.1016/j.gloplacha.2011.06.005, 2012. 4103

Gardner, A. S., Moholdt, G., Wouters, B., Wolken, G. J., Burgess, D. O., Sharp, M. J., Cogley, J. G., Braun, C., and Labine, C.: Sharply increased mass loss from glaciers and ice caps in the Canadian Arctic Archipelago, Nature, 473, 357–360, doi:10.1038/nature10089, 2011. 4103

Graversen, R. G., Mauritsen, T., Tjernstrom, M., Kallen, E., and Svensson, G.: Vertical structure of recent Arctic warming, Nature, 451, 7174., 53–56, doi:10.1038/nature06502, 2008. 4103, 4111, 4112

Hanna, E., Huybrechts, P., Janssens, I., Cappelen, J., Steffen, K., and Stephens, A: Runoff and mass balance of the Greenland ice sheet: 1958–2003, J. Geophys. Res.-Atmos., 110, 13108, doi:10.1029/2004JD005641, 2005. 4110

Hanna, E., Huybrechts, P., Steffen, K., Cappelen, J., Huff, R., Shuman, C., Irvine-Fynn, T., Wise, S., and Griffiths, M.: Increased runoff from melt from the Greenland ice sheet: a response to global warming, J. Climate, 21, 331–341, 2008. 4103

Hanna, E., Jones, J. M., Cappelen, J., Mernild, S. H., Wood, L., Steffen, K., and Huybrechts, P.: The influence of North Atlantic atmospheric and oceanic forcing effects on 1900–2010

Greenland summer climate and ice melt/runoff, Int. J. Climatol., doi:10.1002/joc.3475, 2012. 4102, 4103, 4104, 4106, 4111, 4112

Jaiser, R., Dethloff, K., Handorf, D., Rinke, A., and Cohen, J.: Impact of sea ice cover changes on the Northern Hemisphere atmospheric winter circulation, Tellus, 64, 11595, doi:10.3402/tellusa.v64i0.11595, 2012. 4111

Kalnay, E., Kanamitsu, M., Kistler, R., Collins, W., Deaven, D., Gandin, L., Iredell, M., Saha, S., White, G., Woollen, J., Zhu, Y., Leetmaa, A., Reynolds, B., Chelliah, M., Ebisuzaki, W., Higgins, W., Janowiak, J., Mo, K., Ropelewski, C., Wang, J., Jenne, R., and Joseph, D.: The NCEP\/NCAR 40 year reanalysis project, B. Am. Meteorol. Soc., 77, 437–471, 1996. 4105

Kvamsto, N. G., Steinskog, D. J., Stephenson, D. B., and Tjostheim, D. B.: Estimation of trends in extreme melt-season duration at Svalbard, Int. J. Climatol., doi:10.1002/joc.3395, 2011. 4109

Lund, I. A.: Map-pattern typeification by statistical methods. J. Appl Meterol., 2, 56–65, 1963. 4106

Mote, T. L.: Mid-tropospheric Circulation and surface melt on the Greenland ice sheet. Part I: Atmospheric teleconnections, Int. J. Climatol., 18, 111–130, 1998. 4103

Moholdt, G., Nuth, C., Hagen, J. O., and Kohler, J.: Recent elevation changes of Svalbard glaciers derived from ICESat laser altimetry, Remote Sens. Environ., 114, 2756–2767, doi:10.1016/j.rse.2010.06.008, 2010. 4103

Moss, R. H., Edmonds, J. A., Hibbard, K., Manning, M., Rose, S. K., van Vuuren, D. P., Carter, T. R., Emori, S., Kainuma, M., Kram, T., Meehl, G., Mitchell, J., Nakicenovic, N., Riahi, K., Smith, S., Stouffer, R. J., Thomson, A., Weyant, J. and Wilbanks, T.: The next generation of scenarios for climate change research and assessment. Nature, 463, 747–756, 2010. 4122

Mote, T. L.: Greenland surface melt trends 1973–2007: evidence of a large increase in 2007, Geophys. Res. Lett., 34, L22507 5 pp., doi:10.1029/2007GL031976, 2007. 4103

Overland, J. E. and Wang, M.: Large-scale atmospheric circulation changes are associated with the recent loss of Arctic sea ice, Tellus A, 62, 1–9, doi:10.1111/j.1600-0870.2009.00421.x, 2010. 4111

Philipp, A., Bartholy, J., Beck, C., Erpicum, M., Esteban, P., Fettweis, X., Huth, R., James, P., Jourdain, S., Kreienkamp, F., Krennert, T., Lykoudis, S., Michalides, S., Pianko, K., Post, P., Rassilla Álvarez, D., Schiemann, R., Spekat, A., and Tymvios, F. S.: COST733CAT –

a database of weather and circulation type classifications, Phys. Chem. Earth, 35, 360–373, 2010. 4106

Rignot, E. I., Velicogna, van den Broeke, M. R., Monaghan, A., and Lenaerts, J.: Acceleration of the contribution of the Greenland and Antarctic ice sheets to sea level rise, Geophys. Res. Lett., 38, 05503, doi:10.1029/2011GL046583, 2011. 4102

Screen, J. and Simmonds, I.: Erroneous Arctic temperature trends in the ERA-40 reanalysis: a closer look, J. Climate, 24, 2620–2627, doi:10.1175/2010JCLI4054.1, 2011. 4111

Serreze, M., Holland, M., and Stroeve, J.: Perspectives on the Arctic's shrinking sea-ice cover, Science, 315, 1533–1536, doi:10.1126/science.1139426, 2007. 4103, 4111

Serreze, M. C., Barrett, A. P., Stroeve, J. C., Kindig, D. N., and Holland, M. M.: The emergence of surface-based Arctic amplification, The Cryosphere, 3, 11–19, doi:10.5194/tc-3-11-2009, 2009. 4111, 4112

Sharp, M., Burgess, D. O., Cogley, J. G., Ecclestone, M., Labine, C., and Wolken, G.J: Extreme melt on Canada's Arctic ice caps in the 21th century, Geophys. Res. Lett., 38, 11501, doi:10.1029/2011GL047381, 2011. 4103

Tedesco, M., Serreze, M., and Fettweis, X.: Diagnosing the extreme surface melt event over southwestern Greenland in 2007, The Cryosphere, 2, 159–166, doi:10.5194/tc-2-159-2008, 2008a. 4102

Tedesco, M., Fettweis, X., van den Broeke, M. R., van de Wal, R. S. W., and Smeets, C. J. P. P.: Extreme snowmelt in Northern Greenland during summer 2008, Eos Trans. AGU, vol. 89, no. 41, pg. 391, doi:10.1029/2008EO410004, 2008b. 4102

Tedesco, M., Fettweis, X., van den Broeke, M., van de Wal, R., Smeets, P., van de Berg, W. J., Serreze, M. and Box, J.: The role of albedo and accumulation in the 2010 melting record in Greenland, Environ. Res. Lett., vol. 6, no. 1, 6 pp., doi:10.1088/1748-9326/6/1/014005, 2011. 4102, 4103, 4105

Uppala, S.M., Kållberg, P.W., Simmons, A.J., Andrae, U., da Costa Bechtold, V., Fiorino, M., Gibson, J.K., Haseler, J., Hernandez, A., Kelly, G.A., Li, X., Onogi, K., Saarinen, S., Sokka, N., Allan, R.P., Andersson, E., Arpe, K., Balmaseda, M.A., Beljaars, A.C.M., van de Berg, L., Bidlot, J., Bormann, N., Caires, S., Chevallier, F., Dethof, A., Dragosavac, M., Fisher, M., Fuentes, M., Hagemann, S., Hölm, E., Hoskins, B.J., Isaksen, L., Janssen, P.A.E.M., Jenne, R., McNally, A.P., Mahfouf, J.-F., Morcrette, J.-J., Rayner, N.A., Saunders, R.W., Simon, P., Sterl, A., Trenberth, K.E., Untch, A., Vasiljevic, D., Viterbo, P., and Woollen, J.: The ECMWF re-analysis, Q. J. Roy. Meteor. Soc., 131, 2961–3012, doi:10.1256/qj.04.176, 2005. 4104

Van den Broeke, M. R., Bamber, J., Ettema, J., Rignot, E., Schrama, E., van de Berg, W. J., van Meijgaard, E., Velicogna, I., and Wouters, B.: Partitioning recent Greenland mass loss, Science, 326, 984–986, 2009. 4103

Vautard, R. and P. Yiou: Control of recent European surface climate change by atmospheric flow, Geophys. Res. Lett., 36, 22702, doi:10.1029/2009GL040480, 2009. 4107

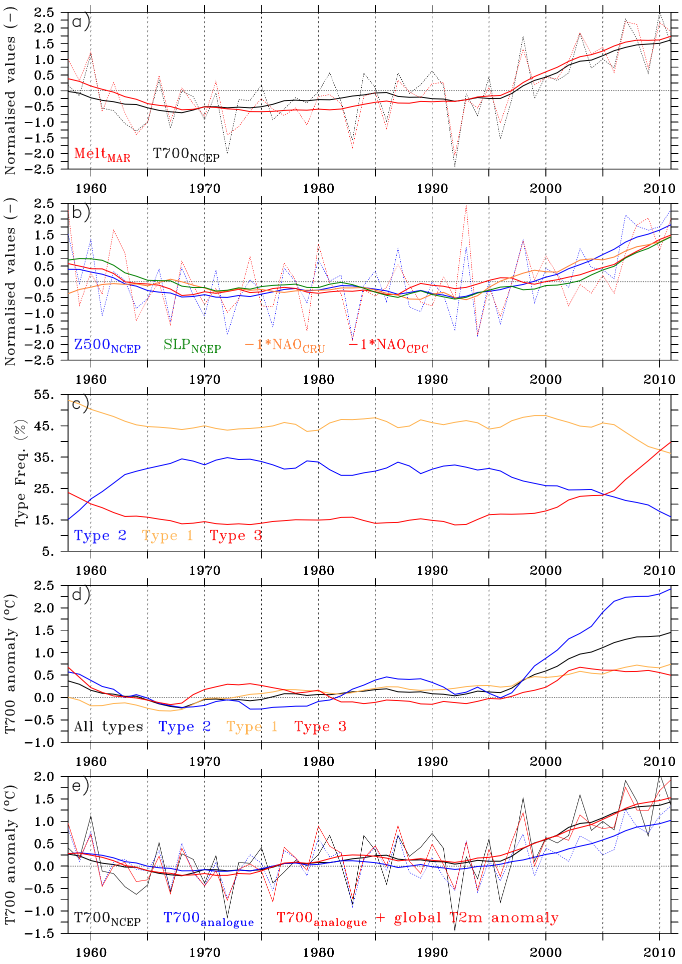

Fig. 1. (Caption on next page.)

Fig. 1. **(a)** Normalized time series of the annual GrIS melt amount simulated by MAR (in red) and of the JJA T700 averaged over the area covering Greenland (70° W $\leq$ longitude $\leq 20^\circ$ W and 60° N $\leq$ latitude $\leq 85^\circ$ N) from the NCEP-NCAR reanalysis (in black). Finally, the solid lines show the 10-yr running mean of the time series. **(b)** Normalized time series of the JJA Z500 averaged over the area covering Greenland (in blue), of the JJA SLP (in green), of the Z500 based NAO index (in red) from the Climate Prediction Center (CPC) of the National Oceanic and Atmospheric Administration (NOAA) and of the SLP-based NAO index (in orange) from the Climate Research Unit (CRU). Here the sign of the NAO indexes time series has been changed to be consistent with the other time series. **(c)** Evolution (in percentage) of the number of occurrences of each circulation class shown in Fig. 3 for each summer from 1958 to 2011. A 10-yr running mean is applied here. **(d)** Time series in °C of the JJA T700 averaged over the area covering Greenland (in black) and of the T700 averaged over the days contained in each type of the CTC. Only 10-yr running means are shown here. Anomalies are relative to the 1961–1990 baseline period. **(e)** Time series in °C of the JJA T700 averaged over the area covering Greenland (in black), of the analogues-based T700 (in blue) and of the analogues-based T700 plus the anomaly of the global annual NCEP-NCAR 2m-temperature (in red) compared with the 1961–1990 mean.

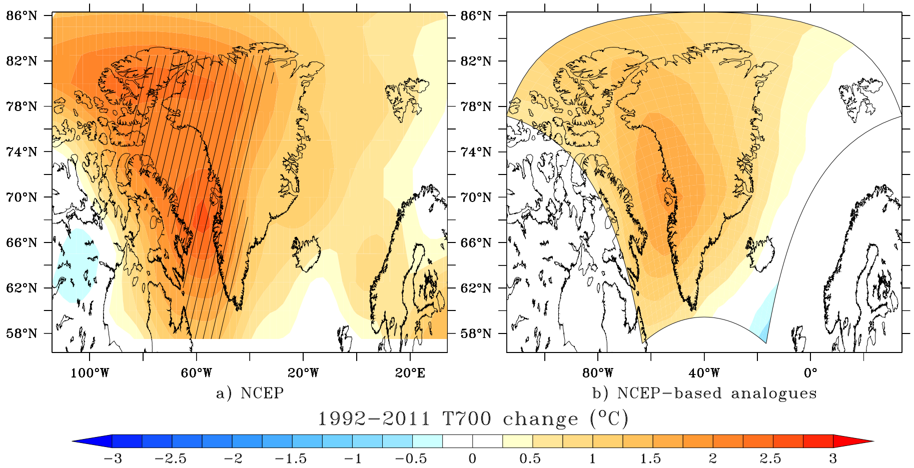

a) NCEP

b) NCEP−based analogues

Fig. 2. (a) The JJA T700 changes over 1992–2011 based on a linear regression using the NCEP-NCAR reanalysis. The areas where the changes are two times above the 1961–1990 JJA T700 standard deviation are hatched. A 10-yr running mean has been applied to the JJA T700 for smoothing the time series before computing the linear regression. **(b)** The same as left but using the NCEP-NCAR-based T700 analogues.

Title Page
Abstract | Introduction
Conclusions | References
Tables | Figures
◀I | ▶I
◀ | ▶
Back | Close
Full Screen / Esc
Printer-friendly Version
Interactive Discussion

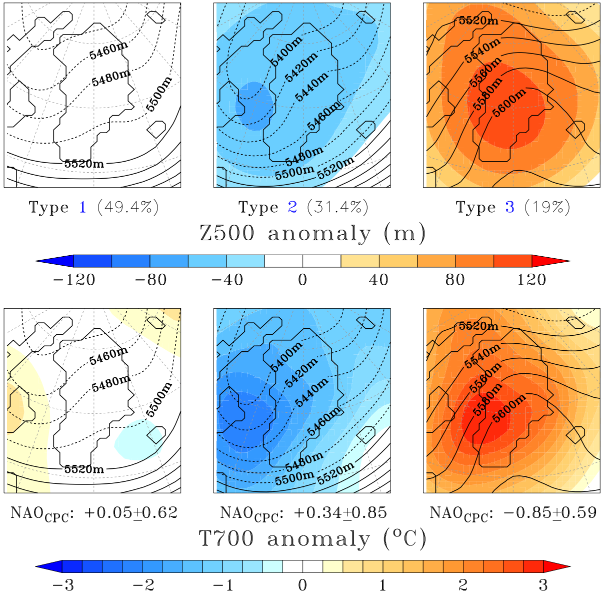

Fig. 3. (Top) The Z500 average over the days categorized into the 8 classes minus the JJA Z500 average over the whole period 1958–2011. The solid lines ($Z500 < 5500\,\text{m}$) and the dashed lines ($Z500 \geq 5500\,\text{m}$) plot the Z500 type-average. For each circulation type, the proportion of days contained in a class compared to the 4968 days of the 1958–2011 JJA months is indicated in brackets. (Below) The lower panels show much the same but for T700. The daily mean NAO index from CPC when the considered circulation type occurs is listed. Both Z500 and T700 fields come here from NCEP-NCAR reanalysis.

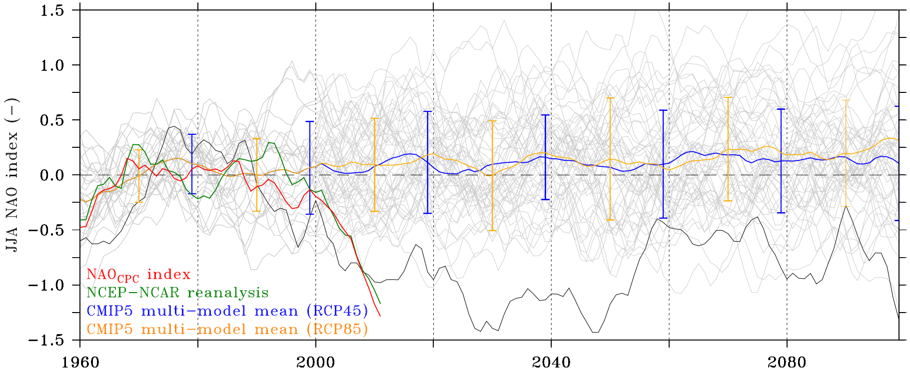

Fig. 4. Time series of the JJA NAO index over 1960–2100. For the NCEP-NCAR reanalysis (in green) and the General Circulation Models (GCMs) from the CMIP5 database, the JJA NAO index is estimated as the standardized (over 1961–1990) difference of the JJA mean sea-level pressure between the Azores (27° W, 39° N) and South-West Iceland (22° W, 64° N). For the CMIP5 GCMs, the Historical scenario is used for both recent (1960–2006) climate conditions and future projections from 2006–2100 based on RCP 4.5 and RCP 8.5 scenarios (Moss et al., 2010). The CMIP5 multi-model mean (composed of 28 GCMs) as well as the standard deviation of the ensemble mean are plotted in blue (RCP 4.5 scenario) and orange (RCP 8.5 scenario). Finally, the JJA NAO index from CPC is plotted in red for comparison.